First Principles Study on the Electronic Structure and Optical Properties of La Doped YB_6 Crystals

Hongbo TANG [1], Qiuyue LI [1], Jian ZHOU [1], Lihua XIAO [2]*, Ping PENG [3]

[1] *Key Laboratory of Jiangxi University for Applied Chemistry and Chemical Biology, Yichun University, Yichun 336000, China*
[2] *School of Materials and Metallurgical Engineering, Guizhou Institute of Technology, Guiyang 550003, China*
[3] *School of Materials Science and Engineering, Hunan University, Changsha, Hunan 410082, China*

crossref http://dx.doi.org/10.5755/j02.ms.25006

Received 03 January 2020; accepted 17 June 2020

We have investigated the optical properties of La (0, 0.125, 0.250) doped YB_6 by means of first-principles calculations within the framework of density functional theory. It was found that electronic and optical properties of YB_6 crystals varied remarkably when Y atoms were replaced with La atoms. Furthermore, with increasing content of La in YB_6 crystals from 12.5 % to 25 % reflectivity and absorption coefficient of near infrared light decreased obviously, while the transmittance was enhanced.

Keywords: YB_6, doped, first principles, optical property.

1. INTRODUCTION

Over the past decades, the first-principles calculations have been used widely to investigate performance of various materials. Relevant findings [1 – 3] have illustrated that the optical properties of these materials could be characterized in terms of dielectric function, reflectivity, absorption and transmittance function, which are mainly related to band structure and electron density. Recently, an increasing attention has been given towards the rare-earth element boride due to interesting structure and optical properties [4, 5]. Among them, yttrium hexaboride (YB_6), an extremely hard, refractory and stable rare-earth hexaboride, has been also applied as solar radiation shielding materials in windows for its high optical absorption coefficient in near-infrared (NIR) range (around 1000 m) and ultraviolet (UV) range (around 350 nm), and high transmittance in visible region. To our knowledge, a lot of researches have been conducted on thermoelectricity [6], super-conductivity [7] and optical performance [8, 9] of YB_6. Even though electronic structure and optical properties of pure YB_6 have been reported by Xiao [8, 9], there are no relevant researches on La doped YB_6. Yttrium and lanthanum belong to one family; they possess many similarities in structure and physicochemical property. Within this paper, band structure, density of states, dielectric function, refractive index, reflectivity, absorption coefficient and transmittance of La doped YB_6 are analyzed and discussed in detail.

2. DETAILS OF CALCULATION

All first-principles calculations were conducted on the basis of density-functional theory incorporated into the Cambridge Serial Total Energy Package (CASTEP) computational code [10]. The interaction between valence electrons and nucleus with positive charges was represented in terms of ultra-soft pseudopotentials [11]. The exchange correlation energy was measured by the generalized gradient approximation (GGA) proposed before [8, 9, 12]. Brillouin zone integration was obtained through the Monkhorst–Pack scheme [13]. Geometry optimization was achieved by convergence thresholds of 2×10^{-5} eV Å^{-1} for total energy and 0.05 eV Å^{-1} for maximum force. It is sufficient to adopt the plane wave cut-off energy of 380 eV and a $6 \times 6 \times 6$ k-point mesh to ensure convergence for the total energy.

In general, YB_6 shows a CsCl-type structure with a Pm3m space group (No. 221), in which Y atom and B_6 octahedron take the sites of cesium and chlorine, respectively. Calculations of the La-doped YB_6 have been performed within a $2 \times 2 \times 2$ supercell of $La_{0.125}Y_{0.875}B_6$, as presented in Fig. 1 b, and a $2 \times 2 \times 1$ supercell of $La_{0.250}Y_{0.750}B_6$ in Fig. 1.

3. RESULTS AND DISCUSSION

3.1. Structural and electronic properties

Y atom occupies the Wyckoff site 1α (0, 0, 0), and B atom locates at the 6*f* (z, 0.5, 0.5) site, with z acting as an internal parameter. According to the previous experimental research [8], the experimental data of α = 4.051 Å and z = 0.1991 Å were set as the initial input for geometry optimization. As many experimental findings reported [8, 14], optimized lattice constants were a =4.052 Å and z = 0.199 Å for pure YB_6.

Fig. 2 shows the calculated total density of states (TDOS) of pure YB_6, $La_{0.125}Y_{0.875}B_6$ and $La_{0.25}Y_{0.75}B_6$, where the Fermi energy level is chosen to be the zero position of the energy scale. As illustrated in the TDOS curves, many bands of two La-doped YB_6 samples cross the Fermi energy level, indicating typical conductor behavior. So it can be concluded that they could be used as conductors like YB_6.

*Corresponding author. Tel.: +86-18275081939.
E-mail address: *xiaolihua@git.edu.cn* (L. Xiao)

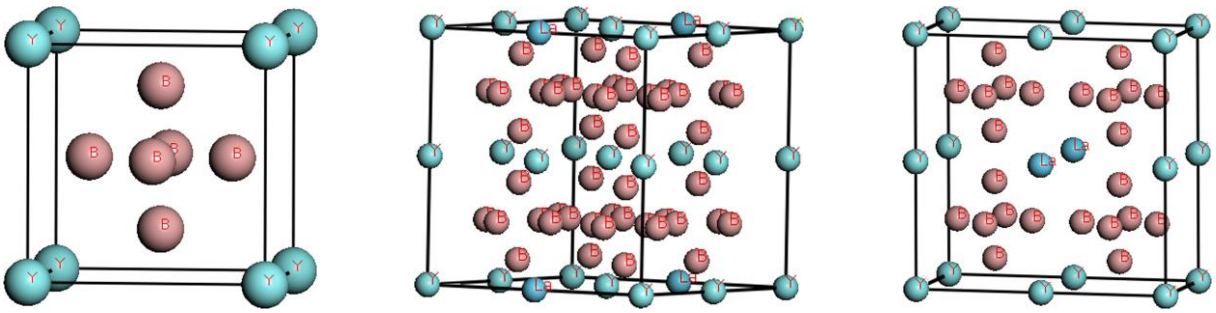

a b c

Fig. 1. Supercell structure: a – YB_6; b – $La_{0.125}Y_{0.875}B_6$; c – $La_{0.25}Y_{0.75}B_6$

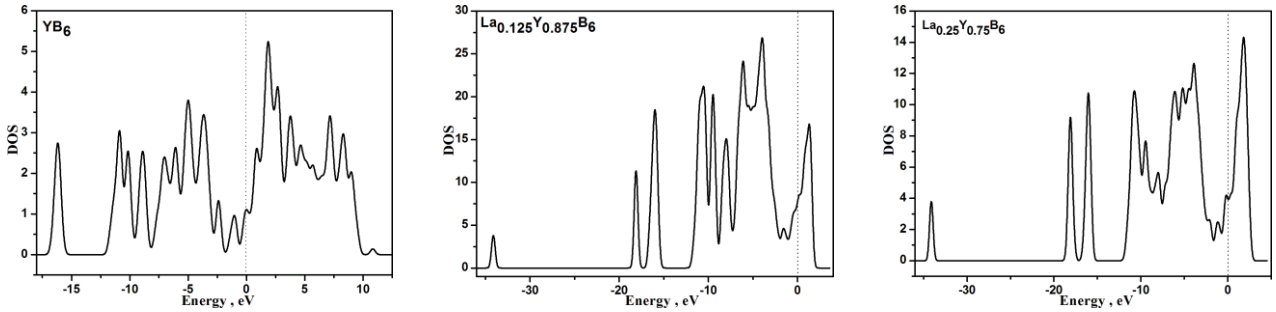

a b c

Fig. 2. Total density of states: a – YB_6; b – $La_{0.125}Y_{0.875}B_6$; c – $La_{0.25}Y_{0.75}B_6$

The partial density of states of YB_6 was obtained, but it is not present here because it is due to its consistency with what has been reported by Xiao et al. [8]. The band structures of pure YB_6, $La_{0.125}Y_{0.875}B_6$ and $La_{0.25}Y_{0.75}B_6$ are plotted in Fig. 3. It can be noticed that the valence bands of the three samples go across the Fermi energy as well, which indicates that the original YB_6, $La_{0.125}Y_{0.875}B_6$ and $La_{0.25}Y_{0.75}B_6$ possess good electrical conductivity.

The above results demonstrate that the YB_6 compounds, no matter pure or doped with low content of the rare-earth element La, show superior conductivity.

3.2. Optical properties

3.2.1. Complex dielectric function

In this section, the complex dielectric function $\varepsilon(\omega)=\varepsilon_1(\omega)+i\varepsilon_2(\omega)$ is usually taken to describe the photon excitation of materials. It has a linear correlation with electromagnetic radiation of materials [15]. The real part (Re) of the dielectric function $\varepsilon_1(\omega)$ describes the dipole polarization intensity and the imaginary part (Im) $\varepsilon_2(\omega)$ is a key parameter in the optical performance. It is related to the electron excitation between occupied and unoccupied bands. Fig. 4 shows the dielectric function of YB_6, $La_{0.125}Y_{0.875}B_6$ and $La_{0.25}Y_{0.75}B_6$.

It can be observed from the real part that there is a transition from the metallic state to the dielectric state for YB_6 and $La_{0.125}Y_{0.875}B_6$, while for $La_{0.25}Y_{0.75}B_6$ no transition zone exists in the curve. The imaginary part of $La_{0.25}Y_{0.75}B_6$ obviously differs from those of the other two sample. This may be ascribed to different electron excitation modes they possess. Thus, it can be concluded that concentration of La in YB_6 has great influence on dielectric function of hexaborides. Then systematical analysis on reflectivity, absorption and transmittance was conducted to compare optical properties of YB_6, $La_{0.125}Y_{0.875}B_6$ and $La_{0.25}Y_{0.75}B_6$.

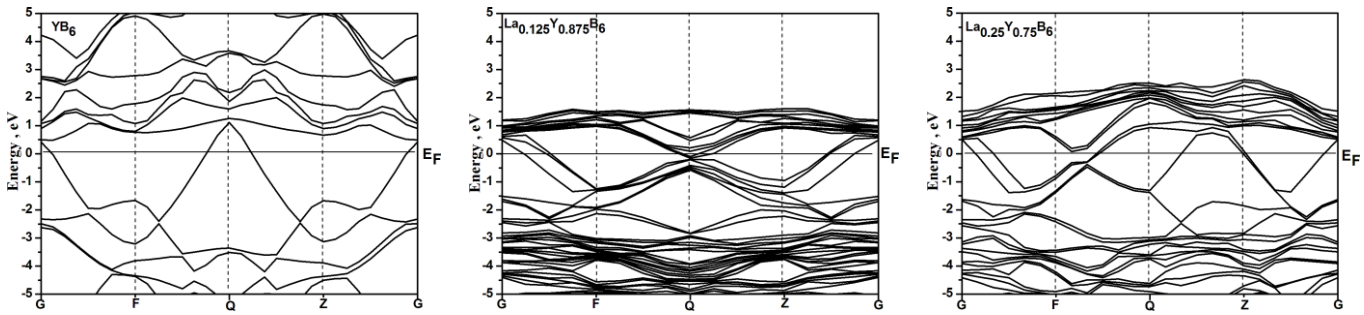

a b c

Fig. 3. Energy band structures: a – YB_6; b – $La_{0.125}Y_{0.875}B_6$; c – $La_{0.25}Y_{0.75}B_6$

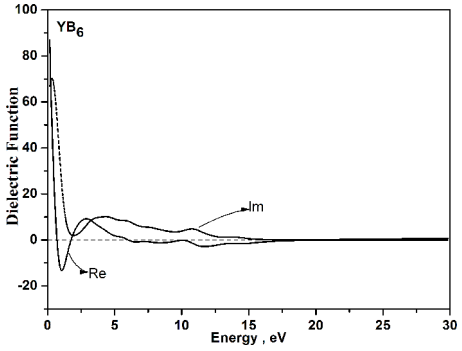

a

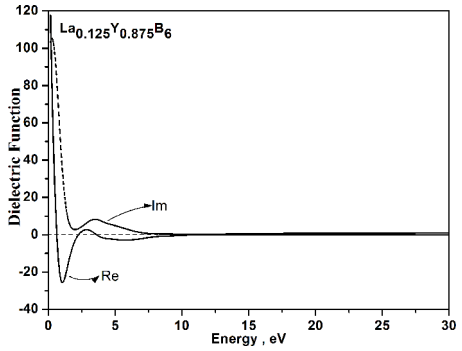

b

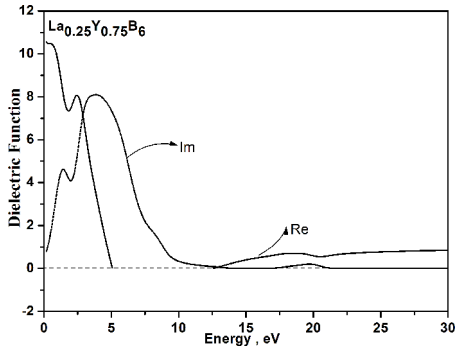

c

Fig. 4. Real part (ε_1) and imaginary part (ε_2) of the complex dielectric constant spectra: a – YB_6; b – $La_{0.125}Y_{0.875}B_6$; c – $La_{0.25}Y_{0.75}B_6$

3.2.2. Reflectivity spectra

Fig. 5 depicts the reflectivity spectra of YB_6, $La_{0.125}Y_{0.875}B_6$ and $La_{0.25}Y_{0.75}B_6$.

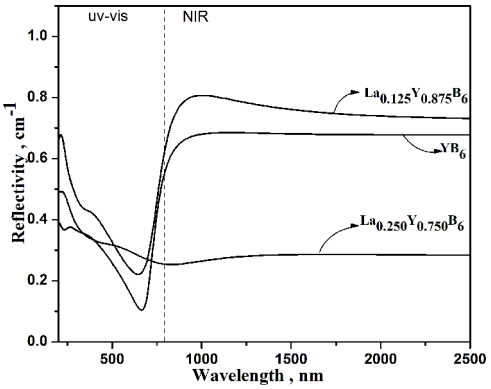

Fig. 5. The reflection spectra of YB_6, $La_{0.125}Y_{0.875}B_6$ and $La_{0.25}Y_{0.75}B_6$

The energy positions of the plasma edge for YB_6 and $La_{0.125}Y_{0.875}B_6$ are V shaped in the visible region, the corresponding minimum values are 695 nm and 685 nm, respectively. The sample $La_{0.25}Y_{0.75}B_6$ shows a relatively low energy position of the plasma edge in the visible region. It also can be observed in Fig. 5 that the maximum reflectivity for YB_6, $La_{0.125}Y_{0.875}B_6$ and $La_{0.25}Y_{0.75}B_6$ in the near infrared region (NIR) is 70 %, 80 % and 28%, respectively. It demonstrates that reflectivity of this kind of materials can be regulated by changing concentration of La.

3.2.3. Absorption spectrum

It can be observed from the absorption spectra of YB_6, $La_{0.125}Y_{0.875}B_6$ and $La_{0.25}Y_{0.75}B_6$ in Fig. 6 that each curve shows a strong absorption peak in the UV region and relatively weak absorption peak in the visible region. Especially for $La_{0.25}Y_{0.75}B_6$ the peak in visible region is far too subtle to be noticed. As observed from the absorption curves of YB_6, a clear absorption valley appears at around 600 nm and there is an absorption peak at around 1100 nm in NIR region. Interestingly, when the La doping content goes up to 12.5 %, the absorption valley shifts toward a higher wavelength. With further increasing the content to 25 %, the corresponding curve is much different from the others. The spectrum shows an absorption peak at visible light region, and then the data changes abruptly and decreases to a minimum value till 2500 nm. As we all know, the position of the absorption valley is always accompanied by the maximum transmission of light. So it can be deduced from this theoretical results that these materials can filter various wavelengths of light from the visible region by tailoring the component.

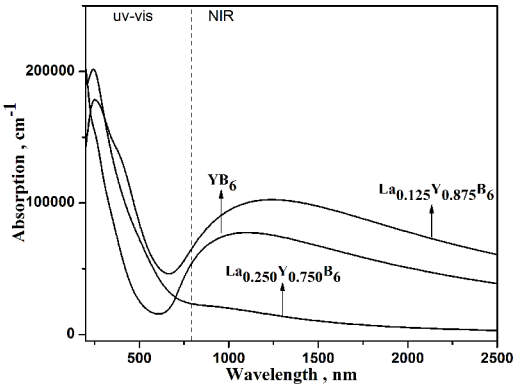

Fig. 6. The absorption spectra of YB_6, $La_{0.125}Y_{0.875}B_6$ and $La_{0.25}Y_{0.75}B_6$

3.2.4. Theoretical transmittance

The theoretical transmittance of YB_6, $La_{0.125}Y_{0.875}B_6$ and $La_{0.25}Y_{0.75}B_6$ films can be obtained according to the Eq. 1 [9]:

$$T = \frac{(1-R^2)\exp(-\alpha d)}{1-R^2\exp(-2\alpha d)}, \quad (1)$$

where T is the theoretical transmittance; R is the reflectivity; α is the absorption coefficient; d is the film thickness. Fig. 7 presents theoretical transmittance of a 50 nm thick film of these samples in the UV-Vis-NIR range. The theoretical transmittance is originated from the

reflection spectrum (Fig. 5) and absorption spectra (Fig. 6) of the samples. It demonstrates that calculated theoretical transmittance values of the compacted films of YB_6, $La_{0.125}Y_{0.875}B_6$ and $La_{0.25}Y_{0.75}B_6$ are different.

Moreover, it can be observed in Fig. 7 that in UV-Vis region, YB_6 and $La_{0.125}Y_{0.875}B_6$ films show transmittance peak at around 695 nm and 685 nm, respectively, but in NIR region they both present weak transmittance. On the contrary, $La_{0.25}Y_{0.75}B_6$ displays high transmittance in the UV-Vis and NIR regions. That is, the transmittance of the La-doped samples in NIR region increases from around 10 % to 50 % apparently by adjusting the content of La from 12.5 % to 25 %.

Based on the above findings, it is found that both YB_6 and $La_{0.125}Y_{0.875}B_6$ are promising solar radiation shielding materials for windows, which require high transmittance for visible light and high blocking effect for near infrared waves [8], while $La_{0.25}Y_{0.75}B_6$ might serve as filter materials. Obviously, the optical tunable characteristic of the ternary materials shows greater potential in practical application than the binary YB_6.

Meanwhile, we noticed some interesting theoretical results, such as similarity in electronic structures and optical properties of YB_6 and $La_{0.125}Y_{0.875}B_6$, and an abrupt leap in the performance when the La content increased to 25 %. These are supposed to be researched and discussed in our future work.

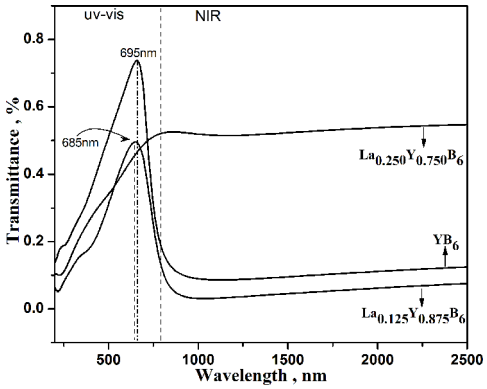

Fig. 7. Theoretical transmittance of 50 nm thick films of YB_6, $La_{0.125}Y_{0.875}B_6$ and $La_{0.25}Y_{0.75}B_6$

4. CONCLUSIONS

In summary, electronic structure and optical characteristics of YB_6, $La_{0.125}Y_{0.875}B_6$ and $La_{0.25}Y_{0.75}B_6$ have been calculated by the density-functional theory within the GGA. The as-obtained lattice constant and optical parameters are in good consistency with reported experimental results. Our findings show that YB_6 and $La_{0.125}Y_{0.875}B_6$ are ideal for the near-infrared absorption/reflectance materials and solar radiation shielding materials for windows which require high transmittance of visible light. As for the $La_{0.25}Y_{0.75}B_6$, it may find potential application in filter materials due to its low absorption/reflectance and high transmittance in NIR.

Acknowledgments

This work is financially supported by the National Natural Science Foundation of China (Nos. 51776046, 61751501), the Foundation of Jiangxi Provincial Education Department (Grant Nos. GJJ161022 and GJJ161035), the Science and Technology Project of Guizhou Province ([2019]1133) and Youth Science and Technology Talent Development Fund in Guizhou Provincial Department of Education ([2018]250).

REFERENCES

1. **Rohlfing, M., Louie, S.G.** Electron-hole Excitations and Optical Spectra from First Principles *Physical Review B* 62 (8) 2000: pp. 4927 – 4944. https://doi.org/10.1103/PhysRevB.62.4927
2. **Norman, P., Agren, H.** First-Principle Quantum Modeling of Optical Power Limiting Materials *Journal of Computational and Theoretical Nanoscience* 1 (4) 2004: pp. 343 – 366. https://doi.org/10.1166/jctn.2004.034
3. **Brik, M.G., Mahlik, S., Jankowski, D., Strak, P., Korona, K.P., Monroy, E., Krukowski, S., Kaminska, A.** Experimental and First-Principles Studies of High-Pressure Effects on the Structural, Electronic, and Optical Properties of Semiconductors and Lanthanide Doped Solids *Japanese Journal of Applied Physics* 56 (5) 2017: pp. 05FA02. https://doi.org/10.7567/JJAP.56.05FA02
4. **Yuan, Y.F., Zhang, L., Hu, L.J., Wang, W., Min, G.H.** Size Effect of Added LaB_6 Particles on Optical Properties of LaB_6/Polymer Composites *Journal of Solid State Chemistry* 184 (12) 2011: pp. 3364 – 3367. https://doi.org/10.1016/j.jssc.2011.10.036
5. **Tang, H.B., Su, Y.C., Hu, T., Liu, S.D., Mu, S.J., Xiao, L.H.** Synergetic Effect of LaB_6 and ITO Nanoparticles on Optical Properties and Thermal Stability of Poly(vinylbutyral) Nanocomposite Films *Applied Physics A-Materials Science & Processing* 117 (4) 2014: pp. 2127 – 2132. https://doi.org/10.1007/s00339-014-8632-8
6. **Lortz, R., Wang, Y., Tutsch, U., Abe, S., Meingast, C., Popovich, P., Knafo, W., Shitsevalova, N., Paderno, Y.B., Junod, A.** Superconductivity Mediated by a Soft Phonon Mode: Specific Heat, Resistivity, Thermal Expansion, and Magnetization of YB_6 *Physical Review B* 73 (2) 2006: pp. 024512. https://doi.org/10.1103/PhysRevB.73.024512
7. **Szabo, P., Girovsky, J., Pribulova, Z., Kacmarcik, J., Mori, T., Samuely, P.** Point-contact Spectroscopy of the Phononic Mechanism of Superconductivity in YB_6 *Superconductor Science & Technology* 26 (4) 2013: pp. 045019. https://doi.org/10.1088/0953-2048/26/4/045019
8. **Xiao, L.H., Su, Y.C., Chen, H.Y., Jiang, M., Liu, S.N., Hu, Z.X., Liu, R.F., Peng, P., Mu, Y.L., Zhu, D.Y.** Study on the Electronic Structure and the Optical Performance of YB_6 by the First-Principles Calculations *AIP Advances* 1 (2) 2014: pp. 022140. https://doi.org/10.1063/1.3602854
9. **Xiao, L.H., Su, Y.C., Zhou, X.Z., Chen, H.Y., Tan, J., Hu, T., Yan, J., Peng, P.** Origins of High Visible Light Transparency and Solar Heat-Shielding Performance in LaB_6 *Applied Physics Letters* 101 (4) 2012: pp. 041913. https://doi.org/10.1063/1.4733386
10. **Segall, M.D., Lindan, P.J.D., Probert, M.J., Pickard, C.J., Hasnip, P.J., Clark, S.J., Payne, M.C.** First-Principles Simulation: Ideas, Illustrations and the

CASTEP Code *Journal of Physics-Condensed Matter* 14 (11) 2002: pp. 2717 – 2744. https://doi.org/10.1088/0953-8984/14/11/301

11. **John P.P., Kieron B., Wang Y.** Generalized Gradient Approximation for the Exchange-Correlation Hole of a Many-Electron System *Physical Review B, Condensed Matter* 54 (23) 1996: pp. 16533 – 16539. https://doi.org/10.1103/PhysRevB.54.16533
12. **Diedrich, C., Grimme, S.** Systematic Investigation of Modern Quantum Chemical Methods to Predict Electronic Circular Dichroism Spectra *Journal of Physical Chemistry A* 107 (14) 2003: pp. 2524 – 2539. https://doi.org/10.1021/jp0275802
13. **Yang, X.P., Chen, J.W., Jiang, H., Dong, J.M.** Chiral Symmetry of Double-Walled Carbon Nanotubes Detected in First-Principles Optical Absorption Spectra *Physical Review B* 69 (19) 2004: pp. 193401. https://doi.org/10.1103/PhysRevB.69.193401
14. **Ning, G.R., Flemming, R.L.** Rietveld Refinement of LaB_6: Data from Mu XRD *Journal of Applied Crystallography* 38 (5) 2005: pp. 757 – 759. https://doi.org/10.1107/S0021889805023344
15. **Xu, Y., Zhang, L.J., Cui, T., Li, Y., Xie, Y., Yu, W., Ma, Y.M., Zou, G.T.** First-Principles Study of the Lattice Dynamics, Thermodynamic Properties and Electron-Phonon Coupling of YB_6 *Physical Review B* 76 (21) 2007: pp. 214103. https://doi.org/10.1103/PhysRevB.76.214103

© Tang et al. *2022* Open Access This article is distributed under the terms of the Creative Commons Attribution 4.0 International License (http://creativecommons.org/licenses/by/4.0/), which permits unrestricted use, distribution, and reproduction in any medium, provided you give appropriate credit to the original author(s) and the source, provide a link to the Creative Commons license, and indicate if changes were made.